

# Effect of $^{18}\text{F}$ -fluorodeoxyglucose extravasation on time taken for tumoral uptake to reach a plateau: animal and clinical PET analyses

Jong Jin Lee<sup>1</sup> · Jin Hwa Chung<sup>2</sup> · Seog-Young Kim<sup>2,3</sup>

Received: 4 April 2016 / Accepted: 24 May 2016 / Published online: 2 June 2016  
© The Japanese Society of Nuclear Medicine 2016

## Abstract

**Objective** The present study aimed to investigate the effect of  $^{18}\text{F}$ -fluorodeoxyglucose (FDG) extravasation on the time taken for tumoral uptake to reach a plateau.

**Methods** For the animal experiment, FDG extravasation was conducted in the tails of HCT116 tumor-bearing xenograft mice models in three groups (no extravasation, 40 % extravasation, and 80 % extravasation;  $n = 5$ , each). Dynamic positron emission tomography (PET) images were acquired over a period of 2 h following injection. Time–activity curves for FDG in the tails and tumors were calculated. For the clinical experiment, 22 patients (male:female, 14:8; age range,  $70.8 \pm 9.2$  years) were subjected to PET/computed tomography (PET/CT) 1 h after the injection of FDG. The inclusion criteria were as follows: (1) submitted to both whole-body and subsequent regional scanning; (2) entire extravasation activity visualized in the whole-body images; (3) tumor visualized on both whole-body and additional regional images; and (4) status of tumor either confirmed by biopsy or clinically

suspected for malignancy. The standardized uptake values (SUVs) of the tumors (on the whole-body and additional PET images) and extravasation sites were recorded.

**Results** There were no significant differences in the time taken for tumoral uptake to reach a plateau and that to reach minimum activity at the extravasation site among the three groups of mice. However, the mean tumoral activity and activity at the extravasation site were negatively correlated at 1 h post-injection. According to the clinical PET findings, the differences in SUV between the whole-body and regional images were not significantly correlated with the interval between injection of FDG and start of whole-body scanning, interval between the start of whole-body scanning and start of regional scanning, extravasation volume, maximum SUV of the extravasation site, or total activity at the extravasation site.

**Conclusions** The time taken for tumoral uptake to reach a plateau is not affected by extravasation, even at extensive degrees. Thus, in routine practice, the imaging time of approximately 60 min post-injection need not be modified even if extravasation is identified. However, tumor SUV may be underestimated in cases of extravasation.

✉ Jong Jin Lee  
jongjin@gmail.com

Jin Hwa Chung  
morality67@naver.com

Seog-Young Kim  
sykim3@amc.seoul.kr

**Keywords** Extravasation · Timing · Time–activity curve · Tumor · FDG · PET

## Introduction

Few studies have been conducted on the extravasation or paravenous injection of radiotracers, because failure to inject a tracer that should have been injected as a bolus can constitute improper practice. Previous studies on extravasation have focused on the potential pitfalls of interpretation of the results [1–5]. The Quantitative Imaging

<sup>1</sup> Department of Nuclear Medicine, Asan Medical Center, University of Ulsan, College of Medicine, 88, Olympic-ro 43-gil, Songpa-gu, Seoul 05505, Korea

<sup>2</sup> Biomedical Research Center, Asan Institute for Life Science, Asan Medical Center, Seoul, Korea

<sup>3</sup> Department of Medicine, University of Ulsan, College of Medicine, Seoul, Korea

Biomarkers Alliance recommends that if  $^{18}\text{F}$ -fluorodeoxyglucose (FDG) extravasation is suspected and the approximate amount of extravasation is expected to be greater than 5 % of the administration activity, the data should be censored if the quantitative result is the primary or secondary endpoint of the study [6].

However, extravasation is not uncommon. Extravasation of FDG during positron emission tomography (PET) occurs in up to 10.5 % of the patients, and at least 31 % of all instances of extravasation go unnoticed, because the antecubital fossa, the most common injection site, is not included in the field of scanning [7]. A correction method was developed to compensate for extravasation in humans, and the authors reported a reduction of bias in the standardized uptake values (SUVs) [8]. Also, an SUV correction formula was developed and tested in a murine model [9]. These correction methods were developed using static images acquired at routine time points. To the best of our knowledge, no study has investigated the effect of extravasation on the optimal image acquisition time. A radiotracer leaking at the extravasation site might continuously infiltrate the systemic blood flow, mainly through the lymphatic or venous systems, in which case, it could be postulated that the leakage of the radiotracer at the extravasation site might result in the continuous infusion of FDG, thus delaying the peak time–activity curve (TAC) of tumoral FDG uptake.

In general, it is recommended that FDG-PET/computed tomography (PET/CT) be conducted at a specific time point (55–75 min) following the injection of FDG [6]. Because the SUVs are affected by the time taken for image acquisition post-injection, maintenance of consistent image acquisition times after the injection of FDG is critical for the accurate interpretation of FDG-PET/CT results [10]. If extravasation leads to delayed tumoral FDG uptake, the optimal time for PET image acquisition might be delayed. The purpose of the present study was to investigate the effect of extravasation on the time taken for tumoral uptake to reach a plateau.

## Materials and methods

### Animal experiments

#### Animal models

All of the procedures and experiments involving animals were performed in accordance with the regulations set forth by the Institutional Animal Care and Use Committee (IACUC) of our institute. Five-week-old male nude mice (*Balb/c nu/nu*, SLC Inc., Shizuoka, Japan), weighing 18–20 g, were examined and acclimated for 1 week under

constant environmental conditions of 20–24 °C, 40–60 % humidity, and a 12-h light/dark cycle. Each mouse was subcutaneously injected with  $5 \times 10^6$  cells/0.2 mL of HCT116 cells in the left upper flank; the cells were in the exponential growth phase. Tumor growth was observed for 2 weeks, and mice with tumor volumes of 80–100 mm<sup>3</sup> were selected for subsequent experiments.

#### Small-animal PET imaging

The mice were fasted overnight (at least 6 h) to avoid myocardial FDG uptake. The xenografted mice were anesthetized with isoflurane (JW pharmaceutical, Seoul, Korea). Following this, 7.4 MBq/0.2 mL FDG was injected into the tail veins of three groups of mice, with deliberate extravasation in two of the three groups. For the non-extravasation group, the entire volume of the radiotracer was smoothly injected without resistance ( $n = 5$ ). For the intermediate extravasation group, the radiotracer was extravasated after the injection of approximately 60 % of the volume into the tail vein ( $n = 5$ ). For the full extravasation group, the radiotracer was extravasated after the injection of approximately 20 % of the volume into the tail vein ( $n = 5$ ; Fig. 1). After injection of the radiotracer, the tails were folded to the right side (contralateral to the tumor) and taped in place using an adhesive tape, so that the distance from the injection site to the bladder remained constant. The mice were moved to the scanner bed 5 min post-injection, and small-animal PET imaging was performed. Dynamic PET images were acquired for 1 h and 55 min using the Concorde Focus 120 scanner (Siemens Healthcare, Erlangen, Germany). The consecutive time frames for acquisition were 30 s  $\times$  1, 60 s  $\times$  4, 180 s  $\times$  1, 300 s  $\times$  6, 450 s  $\times$  1, and 600 s  $\times$  7. During image acquisition, the heart and breathing rates were

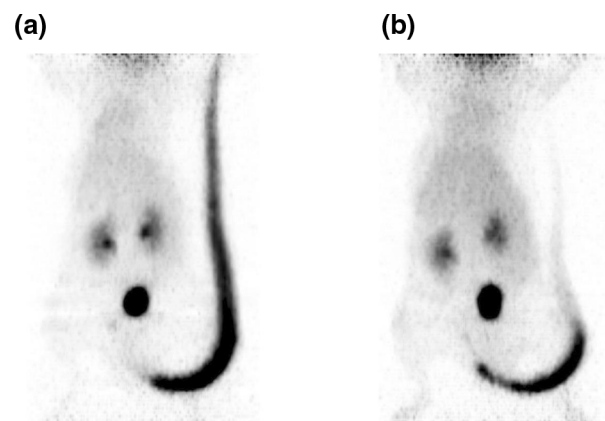


**Fig. 1** Representative cases of extravasation. **a** Full extravasation group (80 %) and **b** intermediate extravasation group (40 %). The images are from the first 30 s frame, acquired 5 min post-injection

monitored using BioVet (m2m Imaging Corporation, Cleveland, OH, USA) to ensure that the breathing rate and body temperature were maintained at 90–130/min and 35–37 °C, respectively. The energy window was set to 350–750 keV, and the coincidence window to 6 ns. The acquired list-mode data were converted into a sinogram by Fourier rebinning (FORE) and subsequently reconstructed using a two-dimensional filtered back projection algorithm. The matrix size of the reconstructed image was set to  $128 \times 128 \times 95$ , and the voxel size to  $0.432 \times 0.432 \times 0.796 \text{ mm}^3$ .

#### *Small-animal PET image analysis*

The TACs and SUVs were analyzed using the ASI Pro software package (Siemens Healthcare, Erlangen, Germany). Regions of interest (ROIs) were marked for the entire extravasation site as well as the tumor. Tumor ROIs were marked excluding internal necrosis, if present. For mice that exhibited no or faint heart visualization at 7200 s, mediastinal blood TACs were also calculated (non-extravasation,  $n = 2$ ; intermediate,  $n = 3$ ; and full,  $n = 3$ ). Maximal intensity projection images were prepared using the InterView FUSION software package (Mediso, Budapest, Hungary; Fig. 1).

#### **Clinical PET analysis**

##### *Subjects*

Experiments involving human subjects were performed in accordance with the Helsinki Declaration and were approved by the institutional review board of our institute. From among the patients who had undergone FDG-PET scans for oncological purposes, subjects who met the following inclusion criteria were enrolled: (1) submitted to both whole-body and subsequent regional scanning; (2) entire extravasation activity visualized in the scanning field; (3) tumor visualized on both whole-body and additional regional images; and (4) status of tumor either confirmed by biopsy or clinically suspected for malignancy.

##### *Image acquisition*

The patients were instructed to avoid strenuous exercise for 24 h prior to FDG-PET/CT examination to minimize the uptake of radiotracer by the muscles. They were also instructed to fast for at least 6 h prior to the injection of FDG. The venous blood glucose concentrations were controlled to ensure levels below 150 mg/dL. The patients were injected with 370–555 MBq of FDG and allowed to rest in a sitting or supine position for 60 min prior to

scanning. Thereafter, they were positioned on the scanner bed with their arms down. Skull base-to-mid thigh PET/CT images (whole-body images) from the upper thighs to the head were acquired using the Discovery STE 8, Discovery PET/CT 690 (GE Healthcare, Waukesha, WI, USA), Biograph TruePoint 16, or Biograph TruePoint 40 (Siemens Healthcare, Germany) scanners. Additional lower-extremity or head-and-neck images were acquired immediately after whole-body imaging, using the same machine.

The voxel sizes of the whole-body and additional lower-extremity images were  $3.91 \times 3.91 \times 5.0 \text{ mm}^3$  for the Biograph TruePoint 16,  $2.98 \times 2.98 \times 5.0 \text{ mm}^3$  for the Biograph TruePoint 40,  $3.91 \times 3.91 \times 3.75 \text{ mm}^3$  for the Discovery STE 8, and  $2.60 \times 2.60 \times 3.75 \text{ mm}^3$  for the Discovery PET/CT 690 scanners. The voxel sizes of the additional head-and-neck images were  $1.95 \times 1.95 \times 5.0 \text{ mm}^3$  for the Biograph TruePoint 16,  $1.48 \times 1.48 \times 3.0 \text{ mm}^3$  for the Biograph TruePoint 40, and  $1.95 \times 1.95 \times 3.75 \text{ mm}^3$  for the Discovery STE 8 and Discovery PET/CT 690 scanners. The voxel sizes of the additional head-and-neck images were set at different values compared to those of the whole-body images, because we wanted to acquire tumor images of higher resolution at the overlapping scanning fields in routine practice. The CT data were used for attenuation correction. Images were acquired at a total of five or six bed-positions. The acquisition times per bed-position were 3 min for the Biograph TruePoint 16 and Discovery STE 8, 2.5 min for the Biograph TruePoint 40, and 2 min for the Discovery PET/CT 690 scanners. Each scanner was routinely calibrated against the dose calibrators and well counters. The measured SUV for the phantom was within the acceptable range of 90–110 %.

##### *Image analysis*

The maximum SUV (SUVmax) of the extravasation site, extravasation volume, and total activity at the extravasation site were recorded. Extravasation volume was defined as the volume of all voxels with SUVs  $\geq 2.5$ . Total activity at the extravasation site on the whole-body PET images was measured using the same method as that for metabolic tumor volume (mean SUV within extravasation volume  $\times$  extravasation volume). Peak SUVs (SUVpeak) of tumors were measured on both the whole-body and additional regional images.

#### **Statistical analysis**

For analysis of the animal PET images, the tumoral mean uptake, activity at the extravasation site, and differences in the mean mediastinal blood pool TAC (according to the extent of extravasation) were examined by repeated

measures analysis of variance. Between-group differences in time taken to reach 90 % of maximum tumoral activity and minimum/0.9 of mediastinal blood pool activity and activity at the extravasation site were examined using the Kruskal–Wallis test. Correlation between tumoral mean activity and activity at the extravasation site and that between the early and late activities at the extravasation site were evaluated using Spearman's rho. In clinical PET image analysis, the correlations of  $\Delta$ SUV (SUV<sub>peak</sub> on additional images – SUV<sub>peak</sub> on whole-body images) and SUV ratio (SUV<sub>peak</sub> on additional images/SUV<sub>peak</sub> on whole-body images) with the interval between injection of FDG and start of whole-body scanning, scan interval (start time of additional scanning – start time of whole-body scanning), SUV<sub>max</sub> of the extravasation site, extravasation volume, and total activity at the extravasation site were evaluated using Spearman's rho. Values of  $P < 0.05$  were considered to be statistically significant. The IBM SPSS Statistics software package (Ver. 21.0, IBM, Armonk, NY) was used for all statistical analyses.

## Results

### Animal PET image analyses

The TACs of tumoral mean uptake and activity at the extravasation site are presented in Fig. 2. No significant intergroup differences were observed in terms of time taken to reach 90 % of the maximum tumoral activity (maximum mean tumoral uptake of all time frames;  $P = 0.170$ ). No significant intergroup differences were observed in terms of time taken to reach minimum/0.9 of mediastinal blood pool activity ( $P = 0.627$ ; Fig. 3). No significant intergroup differences were observed in terms of time taken to reach minimum/0.9 of activity at the extravasation site ( $P = 0.115$ ; Fig. 4). The tumoral mean

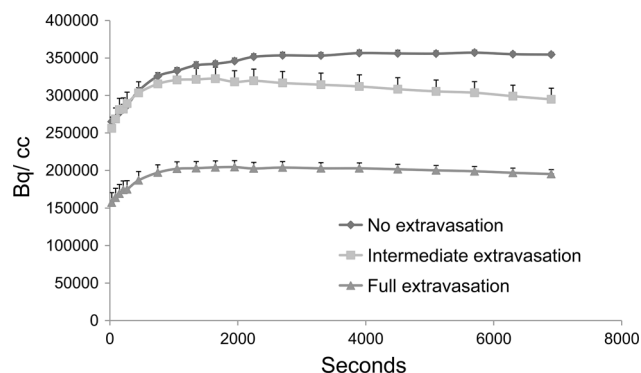


**Fig. 2** Time–activity curve of the tumor. Error bars indicate  $1/5 \times$  standard deviation

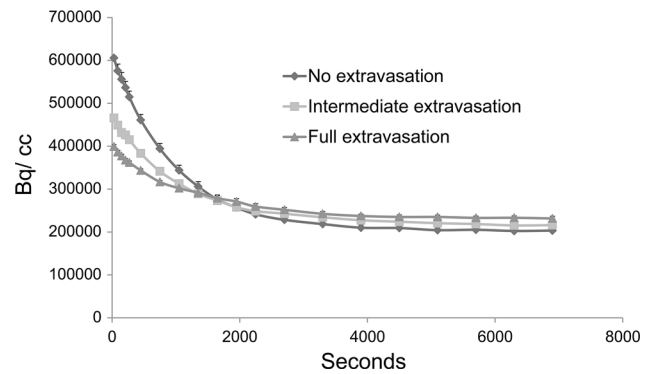


**Fig. 3** Time–activity curve of the mediastinal blood pool. Error bars indicate  $1/5 \times$  standard deviation

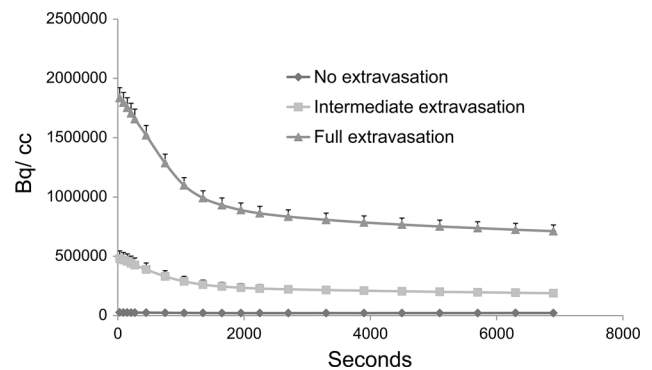


**Fig. 4** Time–activity curve of the tail. Error bars indicate  $1/5 \times$  standard deviation

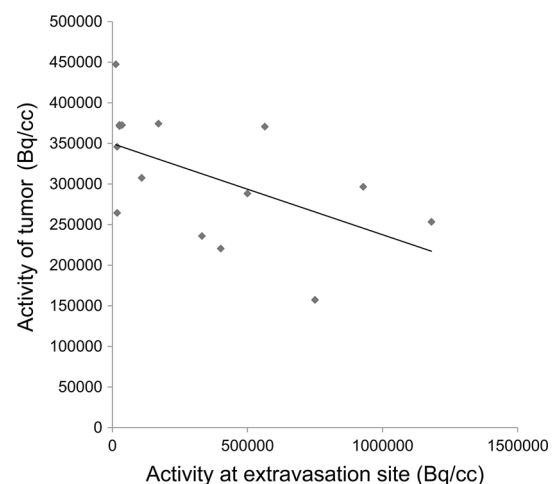


**Fig. 5** Correlation between the activities at the tumor and the extravasation site at the time frame of 3300–3900 s

activity and activity at the extravasation site at the time frame of 3300–3900 s were negatively correlated ( $P = 0.027$ ; Fig. 5). Activities at the extravasation site at time frames 0–30 s and 3300–3900 s were positively correlated ( $P < 0.001$ ; Fig. 6).

### Clinical PET analysis

From among our institutional PET imaging records for the time period between February 2009 and November 2014, 1003 patients had records of FDG-PET/CT images with reports of extravasation. Of the 1003 patients, 110 had undergone additional PET imaging, of whom 20 were excluded, because the extravasation site was not covered in the scanning field. Of the rest, only 26 patients had tumors visualized entirely on both whole-body and additional PET images. After excluding four patients [malignancy not proven upon follow-up examinations (staging PET examination;  $n = 2$ ) and complete metabolic response after treatment (response evaluation PET examination;  $n = 2$ )], 22 patients

(male, 14; female, 8; mean age,  $70.8 \pm 9.2$  years) were finally selected for the study (Figs. 7, 8).

The diagnoses of the patients included in the study were glottic cancer ( $n = 3$ ), tonsil cancer ( $n = 3$ ), tongue cancer ( $n = 2$ ), external auditory canal cancer ( $n = 2$ ), melanoma ( $n = 2$ ), malignancies of unknown origin ( $n = 2$ ), laryngeal cancer ( $n = 1$ ), malignant fibrous histiocytoma ( $n = 1$ ), multiple myeloma ( $n = 1$ ), thyroid anaplastic carcinoma ( $n = 1$ ), thyroid follicular carcinoma ( $n = 1$ ), oral cavity cancer ( $n = 1$ ), lymphoma ( $n = 1$ ), and hepatocellular carcinoma with bone metastasis ( $n = 1$ ). The purposes of PET/CT examinations included staging ( $n = 11$ ), response evaluation ( $n = 4$ ), and restaging ( $n = 7$ ; Table 1).

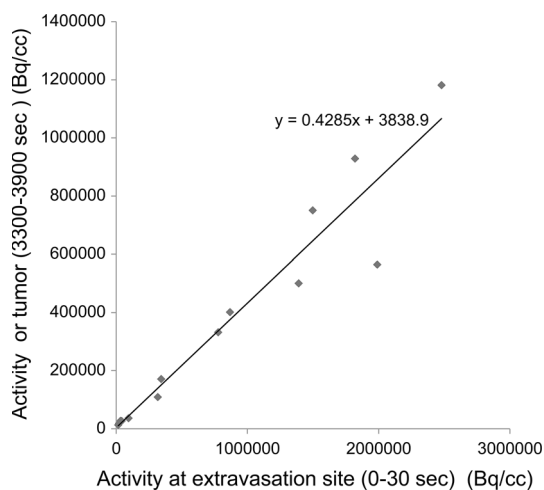


**Fig. 6** Correlation between the activities at the extravasation site at the time frames of 3300–3900 s and 0–30 s

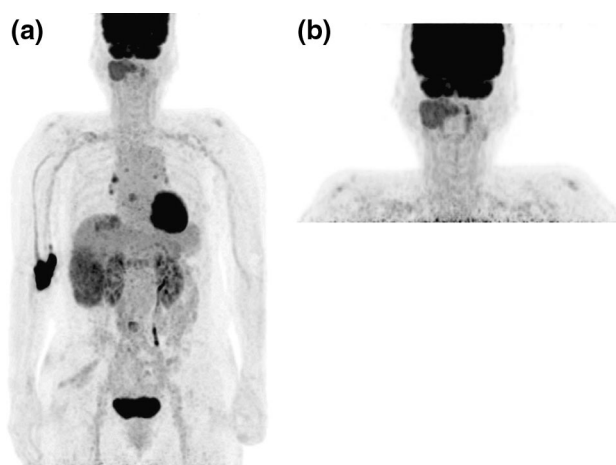


**Fig. 8** Representative image of the clinical positron emission tomography (PET) images. The activity at the extravasation site was 943.11. The peak standard uptake value (SUV<sub>peak</sub>) of tumor changed from 3.7 [whole-body PET (a)] to 3.8 [additional PET (b)]

**Fig. 7** Flow diagram of patient enrollment

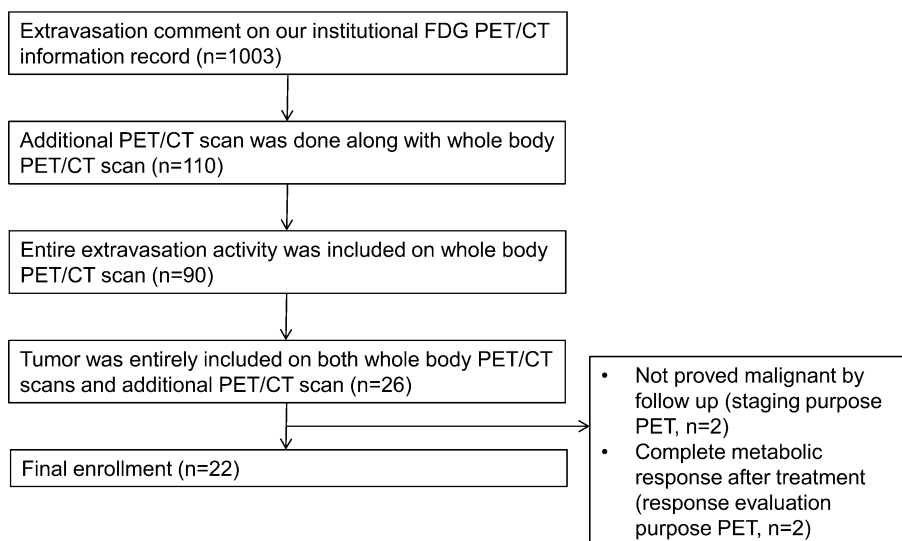


**Table 1** Demographic characteristics of the patients and quantitative parameters of the tumor and extravasation sites

Sex	Age	Injection site	Diagnosis	Purpose of PET/CT	Tumor		Extravasation			Interval (min)				
					SUV peak (WB)	SUV peak (add.)	ΔSUV	SUV ratio	SUV max.	Vol. (ml)	Total activity	Injection–WB scan	WB–add. scan	
1	M	81	Left hand dorsum	Glottic cancer	Staging	12.29	14.76	2.47	1.20	10.05	35.48	163.08	73	25
2	F	67	Right antecubital fossa	External auditory canal tumor	Response evaluation	2.05	2.69	0.64	1.31	12.71	3.10	18.16	79	23
3	M	71	Left antecubital fossa	Larynx cancer, recurred LN	Restaging	3.33	3.94	0.61	1.18	362.28	23.23	725.54	59	29
4	F	53	Left antecubital fossa	Malignant fibrous histiocytoma	Restaging	5.62	5.60	-0.02	1.00	7.99	3.66	15.72	63	28
5	M	79	Right hand dorsum	Tonsil cancer	Response evaluation	4.51	4.85	0.34	1.08	168.61	28.86	325.39	65	15
6	M	59	Left antecubital fossa	External auditory canal tumor	Response evaluation	3.94	4.68	0.74	1.19	4.76	0.53	1.71	67	16
7	F	51	Right hand dorsum	Multiple myeloma	Staging	2.15	2.27	0.12	1.06	232.36	2.19	39.95	53	17
8	F	52	Left hand dorsum	Tongue cancer	Response evaluation	5.34	6.56	1.22	1.23	366.11	13.80	461.20	56	12
9	F	83	Right antecubital fossa	Thyroid anaplastic carcinoma	Staging	18.34	21.78	3.44	1.19	356.76	19.84	608.71	61	13
10	M	72	Right hand dorsum	Glottic cancer	Staging	6.00	6.61	0.61	1.10	805.68	17.98	641.41	56	15
11	M	78	Right hand dorsum	Melanoma	Restaging	7.10	7.38	0.28	1.04	19.05	26.41	128.75	58	23
12	M	69	Right hand dorsum	Glottic cancer	Staging	3.87	4.20	0.33	1.09	356.94	12.41	215.43	53	14
13	M	72	Right hand dorsum	Thyroid follicular carcinoma	Staging	6.39	8.26	1.87	1.29	5.81	0.40	1.51	69	15
14	M	67	Right hand dorsum	Tongue cancer	Restaging	8.02	8.98	0.96	1.12	575.02	22.16	652.32	53	16
15	M	66	Right hand dorsum	MUO lymph node metastasis	Staging	2.08	2.28	0.20	1.10	32.06	36.89	226.63	52	17
16	M	73	Right antecubital fossa	Oral cavity cancer	Restaging	6.93	9.02	2.09	1.30	74.34	2.88	34.35	50	17
17	F	72	Right antecubital fossa	Hepatocellular carcinoma bone metastasis	Staging	3.70	3.80	0.10	1.03	358.20	36.46	943.11	50	17



Table 1 continued

Sex	Age	Injection site	Diagnosis	Purpose of PET/CT	Tumor		Extravasation			Interval (min)				
					SUV peak (WB)	SUV peak (add.)	ΔSUV	SUV ratio	SUV max.	Vol. (ml)	Total activity	Injection-WB scan	WB-add. scan	
18	M	68	Right antecubital fossa	Tonsil cancer	Staging	5.13	5.97	0.84	1.16	6.64	2.25	8.12	70	26
19	M	71	Left hand dorsum	Lymphoma	Restaging	6.47	7.95	1.48	1.23	162.71	33.98	591.70	57	29
20	M	76	Left hand dorsum	Tonsil cancer	Staging	7.64	8.91	1.27	1.17	37.84	58.83	401.16	56	30
21	F	78	Right antecubital fossa	MUO multiple bone metastases	Staging	7.90	11.33	3.43	1.43	8.65	3.09	14.41	57	31
22	F	79	Left hand dorsum	Melanoma	Restaging	2.05	2.51	0.46	1.22	2.75	0.21	0.49	61	29

MUO malignancy of unknown origin, WB whole body, Add. additional, ΔSUV SUVpeak on additional images – SUVpeak on whole-body images, SUV ratio SUVpeak on additional images/ SUVpeak on whole-body images

The mean time from injection of FDG to start of whole-body scanning was  $60.0 \pm 7.8$  min (range 50–79 min); the mean interval between the start of whole-body scanning and start of additional scanning was  $21.0 \pm 6.5$  min. The mean values of ΔSUV and SUV ratios of tumors were not significantly correlated with the interval between injection of FDG and start of whole-body scanning, interval between start of whole-body scanning and start of additional scanning, SUVmax of the extravasation site, extravasation volume, or total activity at the extravasation site.

Discussion

In the animal dynamic PET experiments undertaken in the present study, the time taken for tumoral uptake to reach a plateau was not affected by the extent of extravasation. Analysis of the TACs at the tails indicated that the radiotracer leaked vigorously from the extravasation site, and, approximately 1 h later, the activity of FDG uptake at the tail dropped to half of the initial value and remained constant. This indicates that, even with extensive extravasation, the rate of influx of the radiotracer to the blood stream decreases after a certain time and becomes constant, as observed upon the administration of a bolus or after continuous infusion for 1 h with half the injection dose. The results of evaluation of the blood pool TACs revealed that the actual differences in blood pool TAC were not significantly different from the values that were intuitively expected based on the extravasation site TACs. Although the blood pool concentrations of FDG appeared to be low early after injection and persisted longer in mice with extensive extravasation than in those with no extravasation, no significant differences in TAC were observed among the three groups, which might perhaps have been because of the small sample size or insignificant differences that went undetected. Consequently, the time taken for tumoral uptake to reach a plateau did not differ significantly among the three extravasation groups.

Meanwhile, the tumoral SUV was negatively correlated with the extent of extravasation in the animal study. This result is in concurrence with that observed in a previous study, which reported that paravenous administration affects FDG quantification by 0–50 %, depending on the quality of administration [11]. Therefore, there is a possibility that the SUV might decrease in cases of extravasation, and such cases should, accordingly, be approached with caution.

The metabolic rates of mice and humans differ from each other. For example, the heart rate of mice ranges from 500 to 700 beats/min (bpm) [12] and that of humans ranges from 60 to 100 bpm, at a resting state. Although extravasation in mice may be expected to show a pattern similar to

that observed in humans, the timing might be different. Therefore, we performed an additional retrospective study in humans, considering that prospective studies involving experiments for the evaluation of extravasation in humans are entirely unethical. Based on the results of the present study, the extent of extravasation did not affect the SUVs between approximately 1 and 1.5 h post-injection, which implies that tumor uptake reaches a plateau before 1 h post-injection, regardless of the extent of extravasation. In our animal study, the time taken for tumoral uptake to reach a plateau remained unaffected even at extensive degrees of extravasation (80 %). Extravasation >50 % is an extreme experimental condition, which is unlikely to occur in clinical practice. Therefore, in cases of extravasation, the usual imaging time of 60 min after the injection of radiotracer need not be modified in routine practice.

The results of the present study are clinically significant in that they might help resolve concerns about optimal timing, if appropriate correction methods for tumoral uptake are developed in cases of extravasation. At the very least, our results might help clarify the optimal image acquisition time for PET, in instances where retest is practically impossible. Also, our FDG-PET findings might also be of relevance to other nuclear medicine imaging modalities, including bone scans, which are usually conducted 2 h or later following the injecting of radiotracers.

The present study does, however, have some limitations. First, in clinical PET image analysis of tumoral uptake, we evaluated the SUV<sub>peak</sub>, because the voxel sizes for whole-body and regional PET image acquisitions were not the same. We routinely acquire regional PET images with smaller voxel sizes to visualize the lesions more closely. Since differences in voxel sizes can lead to differences in the SUV calculations [11], we analyzed the SUV<sub>peak</sub> instead of the SUV<sub>max</sub> for the reason that the SUV<sub>peak</sub> is more reproducible and less sensitive to noise than the SUV<sub>max</sub> [13]. Likewise, we analyzed the mean SUV in animal tumoral uptake analysis, because the SUV<sub>max</sub> was very sensitive to noise. Second, the sample size for clinical PET analysis was not determined statistically, which might have resulted in reduced power; therefore, the sample size might have been too small to detect the differences in SUV<sub>peak</sub>. However, the results of our animal experiments support our major findings. Third, in our clinical PET analysis, we were unable to include a non-extravasation group for comparison of the results observed with our study subjects. Selection of patients with non-extravasation was not practically feasible, because the sample size was relatively small ( $n = 22$ ) in comparison with the number of factors involved in tumoral FDG uptake. However, since the volume and total activity of extravasation showed a wide range of distribution (0.21–58.83 mm<sup>3</sup> and 0.49–943.11, respectively), we believe that intragroup

analyses of extravasation might be adequate for the identification of the correlation between tumoral FDG uptake and extravasation activity. Fourth, since the SUVs at the extravasation sites were extraordinarily high, we cannot rule out the possibility of SUV saturation, which might have caused underestimation of the activity at the extravasation site. Fifth, in our animal study, the TACs could not be recorded immediately post-injection. This loss of data in the first 5 min following injection was inevitable, because we were unable to create an extravasation model for image acquisition with the animals lying down on the PET scanner bed. Nevertheless, we do not believe that this omission would affect our major findings, because the time of interest was more than 1 h post-injection.

## Conclusion

The time taken for tumoral uptake to reach a plateau is not affected by extravasation, even in cases of extensive extravasation. Thus, in routine practice, the imaging time of approximately 60 min after FDG injection need not be modified even if the occurrence of extravasation is identified. However, the tumor SUVs may be underestimated in cases of extravasation.

## Compliance with ethical standards

**Conflict of interest** None to declare.

**Research involving human participants and/or animals** This study was performed in accordance with the Helsinki Declaration and was approved by the Institutional Review Board of Asan Medical Center (S2016-0178). Each procedure and animal experiment followed regulations set forth by the Institutional Animal Care and Use Committee (IACUC) at the Asan Medical Center.

**Informed consent** Informed consent was waived by the Institutional Review Board of Asan Medical Center.

## References

1. Pitman AG, Binns DS, Ciavarella F, Hicks RJ. Inadvertent 2-deoxy-2-[<sup>18</sup>F]fluoro-D-glucose lymphoscintigraphy: a potential pitfall characterized by hybrid PET-CT. *Mol Imaging Biol.* 2002;4:276–8.
2. Chiang SB, Rebenstock A, Guan L, Burns J, Alavi A, Zhuang H. Potential false-positive FDG PET imaging caused by subcutaneous radiotracer infiltration. *Clin Nucl Med.* 2003;28:786–8.
3. Manohar K, Agrawal K, Bhattacharya A, Mittal BR. New axillary lymph nodal F-18 fluoro-deoxy glucose uptake in an interim positron emission tomography scan—not always a sign of disease progression. *Indian J Nucl Med.* 2011;26:192–3.
4. Wagner T, Brucher N, Julian A, Hitzel A. A false-positive finding in therapeutic evaluation: hypermetabolic axillary lymph node in a lymphoma patient following FDG extravasation. *Nucl Med Rev Cent East Eur.* 2011;14:109–11.



5. Sonoda LI, Ghosh-Ray S, Sanghera B, Dickson J, Wong WL. FDG injection site extravasation: potential pitfall of misinterpretation and missing metastases. *Clin Nucl Med*. 2012;37:1115–6.
6. Quantitative FDG-PET Technical Committee. UPICT oncology FDG-PET CT protocol. Quantitative Imaging Biomarkers Alliance. [http://qibawiki.rsna.org/images/d/de/UPICT\\_Oncologic\\_FDGPETCTProtocol\\_6-07-13.pdf](http://qibawiki.rsna.org/images/d/de/UPICT_Oncologic_FDGPETCTProtocol_6-07-13.pdf). Accessed 28 Mar 2016.
7. Osman MM, Muzaffar R, Altinyay ME, Teymouri C. FDG dose extravasations in PET/CT: frequency and impact on SUV measurements. *Front Oncol*. 2011;1:41.
8. Silva-Rodriguez J, Aguiar P, Sanchez M, Mosquera J, Luna-Vega V, Cortes J, et al. Correction for FDG PET dose extravasations: Monte Carlo validation and quantitative evaluation of patient studies. *Med Phys*. 2014;41:052502.
9. Lasnon C, Dugue AE, Briand M, Dutoit S, Aide N. Quantifying and correcting for tail vein extravasation in small animal PET scans in cancer research: is there an impact on therapy assessment? *EJNMMI Res*. 2015;5:61.
10. Lowe VJ, DeLong DM, Hoffman JM, Coleman RE. Optimum scanning protocol for FDG-PET evaluation of pulmonary malignancy. *J Nucl Med*. 1995;36:883–7.
11. Boellaard R. Standards for PET image acquisition and quantitative data analysis. *J Nucl Med*. 2009;50(Suppl 1):11S–20S.
12. Ho D, Zhao X, Gao S, Hong C, Vatner DE, Vatner SF. Heart rate and electrocardiography monitoring in mice. *Curr Protoc Mouse Biol*. 2011;1:123–39.
13. Wahl RL, Jacene H, Kasamon Y, Lodge MA. From RECIST to PERCIST: evolving considerations for PET response criteria in solid tumors. *J Nucl Med*. 2009;50(Suppl 1):122S–50S.